VOL. 4, NO. 2 HVAC&R RESEARCH APRIL 1998

Infiltration Load in Cold Rooms

Moustafa M. Elsayed
Member ASHRAE

A two dimensional model was developed to predict the infiltration load to a cold room through its doorway. The governing equations were derived and transformed into dimensionless form. The model showed that the infiltration load to a cold room depends on three dimensionless parameters: the Grashof number of the cold room, the aspect ratio of the room (height to width), and the opening ratio (height of doorway to height of the room). A finite difference technique with a control volume approach was used to solve the governing equations. Staggered grids were used, extending them beyond the doorway to account for the air motion outside the cold room. A SIMPLER algorithm, with finite difference formulation was used to solve the governing equations together with their boundary conditions. The model was used to predict the flow pattern and the temperature distribution in the cold room due to the infiltration through the doorway. The results were also utilized to study the variation of the rate of infiltration and the doorway flow factor with the time measured from the moment the door was opened. The results are presented for the Grashof number from 10^5 to 10^7 and 10^{10}, and opening ratios of 0.5 to 0.25. Comparisons of results with those in the literature are presented. The good agreement of the simulation with the experiments suggests that the present model is valid for the type of flows compared.

INTRODUCTION

Infiltration load through doorways represents a major fraction of refrigeration load in cold stores, especially when these stores are used for short term storage or for distribution operation. This infiltration load is determined in terms of the rate of infiltration air through the doorway of a cold room and the conditions of the air inside and outside the room, i.e.

$$Q = \dot{m}_{inf}(h_\infty - h_c) \tag{1}$$

where h_∞ and h_c are the enthalpy of the infiltration air and cold air, respectively. The uncertainty in the calculation of the infiltration load Q is only due to the uncertainty in the calculation of $\dot{m}_{inf}$. The determination of $\dot{m}_{inf}$ depends on several factors. These include the duration for which the door is kept open, the frequency of opening the door and the effectiveness of doorway protective device.

A well accepted relation to determine $\dot{m}_{inf}$ is given in the following form (ASHRAE 1994)

$$\dot{m}_{inf} = \dot{m}_{ss} D_t D_f (1 - E) \tag{2}$$

where D_t is the doorway open-time factor, D_f is the doorway flow factor, E is the effectiveness of doorway protective device, and $\dot{m}_{ss}$ is the steady-state flow rate of infiltration air for a permanently open doorway.

Moustafa M. Elsayed is a professor of mechanical engineering at Kuwait University, Safat, Kuwait.

Several correlations are available in the literature to estimate $\dot{m}_{ss}$. The most recognizable one is that of Gosney and Olama (1975), recommended by ASHRAE (1994). This relation gives $\dot{m}_{ss}$ by the following expression

$$\frac{\dot{m}_{ss}}{L} = 0.221\rho_c\left(1-\frac{\rho_\infty}{\rho_c}\right)^{0.5} g^{0.5} H_1^{1.5}\left[\frac{2}{1+(\rho_c/\rho_\infty)^{1/3}}\right]^{1.5} \tag{3}$$

where L is the length of the doorway, H_1 is its height, ρ is the density of air, and the subscripts c and ∞ refer to cold air and infiltration air, respectively. The above correlation is derived using non-viscous, one dimensional analysis and a small-scale experimental model using CO_2 and air to represent the differing densities that would be encountered as a result of temperature differences.

In an independent study, Jones et al. (1983) studied the transfer of moisture to a conditioned space due to infiltration air. Their results are expressed here in the following form

$$\frac{\dot{m}_{ss}}{L} = 0.173\bar{\rho}\left[gH_1\left(\frac{T_\infty}{T_c}-\frac{T_c}{T_\infty}\right)\right]^{0.5} H_1 \tag{4}$$

where T_∞ and T_c is in kelvin and $\bar{\rho}$ is the air density calculated at the arithmetic mean temperature of T_∞ and T_c. The above correlation is derived using simple one-dimensional convection analysis and experimental measurements for the moisture transfer.

Another crude correlation is the correlation reported by Cole (1984) that yields

$$\frac{\dot{m}_{ss}}{L} = 0.0603\bar{\rho}(T_\infty - T_c)^{0.5} H_1^{1.5} \tag{5}$$

where $\bar{\rho}$ is the average density of air outside and inside the cold room.

The above correlations have several drawbacks. First, the correlations have been derived assuming non-viscous one-dimensional flow (Equations 3 and 4) or zero dimensional flow (Equation 5). Second, the correlations do not account for the dimensions (width and height of the cold room) and the relative value of these dimensions to the height of the door. Third, the experimental works used to develop Equations 3 and 4 are restricted to the geometrical dimensions of laboratory setup. These correlations may be questionable if applied to actual geometry due to differences in the value of the Grashof number of the experiment compared to the real cold room.

The objective of the present work was to develop a two-dimensional viscous model to predict the infiltration load in cold rooms. The model was designed to:

1. Check the accuracy of the currently used correlations from Equations (3), (4), and (5)
2. Study the effect of changing the Grashof number and the ratio of the doorway height to the room height on the infiltration load
3. Predict the value of the doorway flow factor to cold rooms.

GOVERNING EQUATIONS AND BOUNDARY CONDITIONS

Consider the cross section of the cold store shown in Figure 1. The store has a height H, a width B, and a door height H_1. When the door is closed, the air temperature in the store and the temperatures of all walls were maintained at T_c with the thermostat in the store. The air outside the door of the store was at temperature T_∞. When the door is open, warm air at T_∞ infiltrates

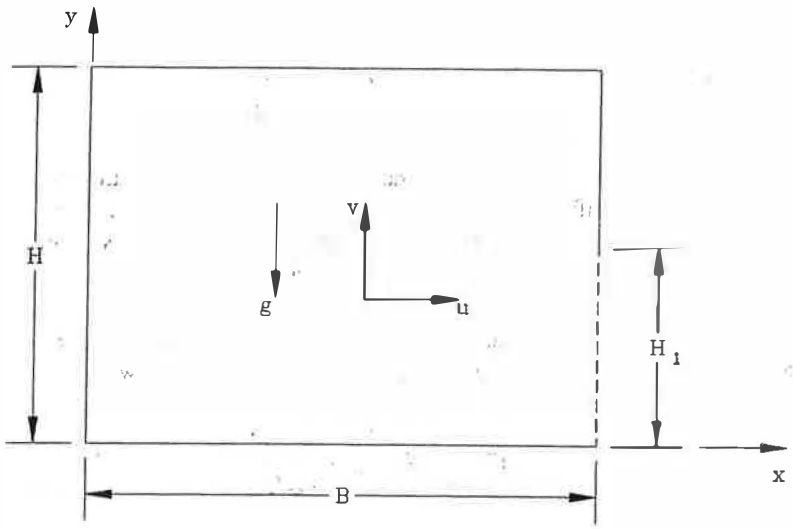

Figure 1. Geometry of cold room

into the store. To derive the governing equations that predict the air motion through the door and also to calculate the part of the cooling load due to this infiltrated air, the following assumptions were made:

- The door opening is the full length of the store
- The length of the store is large enough to allow two-dimensional analysis
- All air properties are constant except its density which changes with temperature, in accordance with the Boussinesq approximation
- All walls are isothermal at T_c

The governing equations then take the following form

$$\frac{\partial u}{\partial x} + \frac{\partial v}{\partial y} = 0 \tag{6}$$

$$\frac{\partial u}{\partial t} + u\frac{\partial u}{\partial x} + v\frac{\partial u}{\partial y} = \frac{\mu}{\rho}\left(\frac{\partial^2 u}{\partial x^2} + \frac{\partial^2 u}{\partial y^2}\right) - \frac{1}{\rho}\frac{\partial p}{\partial x} \tag{7}$$

$$\frac{\partial v}{\partial t} + u\frac{\partial v}{\partial x} + v\frac{\partial v}{\partial y} = \frac{\mu}{\rho}\left(\frac{\partial^2 v}{\partial x^2} + \frac{\partial^2 v}{\partial y^2}\right) + g\beta(T - T_\infty) - \frac{1}{\rho}\frac{\partial p}{\partial y} \tag{8}$$

$$\frac{\partial T}{\partial t} + u\frac{\partial T}{\partial x} + v\frac{\partial T}{\partial y} = \frac{k}{\rho C_p}\left(\frac{\partial^2 T}{\partial x^2} + \frac{\partial^2 T}{\partial y^2}\right) \tag{9}$$

where x and y are the distances along the coordinates x and y, respectively (see Figure 1), u and v are, respectively, the velocity components in the x and y directions; p is the pressure, t is the time measured from the instance of opening the door; T is the temperature, and ρ, C_p, k, μ, and β are the properties of air, as described in the nomenclature.

To generalize the solution of the governing equations, the following dimensionless variables were introduced

$$\left.\begin{aligned} X = \frac{x}{H}, Y = \frac{y}{H}, U = \frac{u}{u_{ref}}, V = \frac{v}{u_{ref}} \\ \theta = \frac{T - T_\infty}{T_\infty - T_c}, P = \frac{p - p_\infty}{\rho u_{ref}^2}, \tau = \frac{t u_{ref}}{H} \end{aligned}\right\} \tag{10}$$

where the reference velocity u_{ref} is given by

$$u_{ref} = \sqrt{g\beta\Delta T_{ref} H} \tag{11}$$

Using these dimensionless variables, the governing equations are reduced to the following

$$\frac{\partial U}{\partial X} + \frac{\partial V}{\partial Y} = 0 \tag{12}$$

$$\frac{\partial U}{\partial \tau} + U\frac{\partial U}{\partial X} + V\frac{\partial U}{\partial Y} = \mathrm{Gr}^{-1/2}\left(\frac{\partial^2 U}{\partial X^2} + \frac{\partial^2 U}{\partial Y^2}\right) - \frac{\partial P}{\partial X} \tag{13}$$

$$\frac{\partial V}{\partial \tau} + U\frac{\partial V}{\partial X} + V\frac{\partial V}{\partial Y} = \mathrm{Gr}^{-1/2}\left(\frac{\partial^2 V}{\partial X^2} + \frac{\partial^2 V}{\partial Y^2}\right) + \theta - \frac{\partial P}{\partial Y} \tag{14}$$

$$\frac{\partial \theta}{\partial \tau} + U\frac{\partial \theta}{\partial X} + V\frac{\partial \theta}{\partial Y} = \frac{\mathrm{Gr}^{-1/2}}{\mathrm{Pr}}\left(\frac{\partial^2 \theta}{\partial X^2} + \frac{\partial^2 \theta}{\partial Y^2}\right) \tag{15}$$

where the Prandtl number Pr and the Grashof number Gr are given by the following expressions

$$\mathrm{Pr} = \frac{\mu C_p}{k}, \qquad \mathrm{Gr} = \frac{\rho^2 g\beta(T_\infty - T_c)H^3}{\mu^2} \tag{16}$$

The dimensional governing equations, Equation (1) to (4), are subject to the following initial conditions

$$\left.\begin{aligned} t < 0: \ [[T]]_c = T_c \ , \ [[T]]_\infty = T_\infty \\ [[u]]_c = 0 \ , \ [[u]]_\infty = 0 \\ [[v]]_c = 0 \ , \ [[u]]_\infty = 0 \end{aligned}\right\} \tag{17}$$

where $[[\ ]]_c$ means "over the domain in the cold store," and $[[\ ]]_\infty$ means "over the domain outside the store." At $t = 0$ the door of the store was open, thus the boundary conditions became

$$t \geq 0:\ x \to \infty \text{ and/or } y \to \infty,\ T = T_\infty,\ u = v = 0$$
$$\left.\begin{array}{ll} x = 0, & 0 \leq y \leq H \\ x = B, & H_1 \leq y \leq H \end{array}\right\} T = T_c$$
$$\left.\begin{array}{ll} y = 0, & 0 \leq x \leq B \\ y = H, & 0 \leq x \leq B \end{array}\right\} u = v = 0 \qquad (18)$$

In dimensionless form these initial and boundary conditions are reduced to the following

$$\left.\begin{array}{l} \tau < 0:\ [[\theta]]_c = -1,\quad [[\theta]]_\infty = 0 \\ [[U]]_c = [[U]]_\infty = 0 \\ [[V]]_c = [[V]]_\infty = 0 \end{array}\right\} \qquad (19)$$

$$\tau \geq 0:\ X \to \infty \text{ and/or } Y \to \infty,\ \theta = 0,\ U = V = 0$$
$$\left.\begin{array}{ll} X = 0, & 0 \leq Y \leq 1 \\ X = \dfrac{1}{AR}, & OR \leq Y \leq 1 \\ Y = 0, & 0 \leq X \leq \dfrac{1}{AR} \\ Y = 1, & 0 \leq X \leq \dfrac{1}{AR} \end{array}\right\} \begin{array}{l} \theta = -1 \\ U = V = 0 \end{array} \qquad (20)$$

where AR and OR are, respectively, the aspect ratio of the store and its opening ratio, i.e.

$$AR = \frac{H}{B} = \frac{1}{\bar{B}}, \qquad OR = \frac{H_1}{H} \qquad (21)$$

CALCULATION OF COOLING LOAD DUE TO INFILTRATION

The rate of infiltrated air to the store through the door opening is estimated at any instant of time t as follows

$$\frac{\dot{m}_a}{L} = \int_0^{H_1} [(\rho u\, dy)_{x = B}]^+ \qquad (22)$$

where the superscript + indicates that only positive values of the integrand is considered when making the integration, and L is the length of the store. Using dimensionless parameters, the above equation becomes

$$\dot{M}_a = \frac{\dot{m}_a}{\rho u_{ref} LH} = \int_0^{OR} (U dY)^+_{x = \bar{B}} \qquad (23)$$

where $\dot{M}_a$ is the dimensionless rate of infiltrated air.

The sensible part Q_s of the infiltration cooling load is estimated by the following integration

$$\frac{Q_s}{L} = -\int_0^{H_1} [\rho u C_p (T - T_\infty) dy]_{x=B} - \int_0^{H_1} \left[-\left(k \frac{\partial T}{\partial x} \right) dy \right]_{x=B} \tag{24}$$

Using dimensionless parameters, this becomes

$$\frac{Q_s}{\rho u_{ref} C_p (T_\infty - T_c) LH} = -\int_0^{OR} (U\theta dY)_{X=\bar{B}} + \frac{1}{\mathrm{Gr}^{1/2}\mathrm{Pr}} \int_0^{OR} \left(\frac{\partial \theta}{\partial X} dY \right)_{x=\bar{B}} \tag{25}$$

Conventionally, Q_s is estimated using a modified rate $\dot{m}$ of infiltrated air in the following equation

$$Q_s = \dot{m} C_p (T_\infty - T_c) \tag{26}$$

Using Equations (25) and (26), the dimensionless modified rate of infiltrated air will then be given by

$$\dot{M} = \frac{\dot{m}}{\rho u_{ref} LH} = -\int_o^{OR} (U\theta dY)_{x=\bar{B}} + \frac{1}{\mathrm{Gr}^{1/2}\mathrm{Pr}} \int_o^{OR} \left(\frac{d\theta}{dX} dY \right)_{x=\bar{B}} \tag{27}$$

Comparing Equations (27) and (23) to one another shows that Equation (27) reduces to Equation (23) when the heat conduction at the doorway is neglected and if the inflow at the doorway is assumed at T_∞ (i.e. $\theta = 0$) and the outgoing flow is assumed at T_c (i.e. $\theta = -1$).

If Q_L is the part of infiltration cooling load which is latent, then the sensible heat factor SHF of the infiltration process is given by

$$\mathrm{SHF} = \frac{Q_s}{Q_s + Q_L} \tag{28}$$

Rearranging, Q_L can be expressed as follows

$$Q_L = \frac{(1 - \mathrm{SHF})}{\mathrm{SHF}} Q_s \tag{29}$$

The SHF in the above equation is determined in terms of the conditions inside and outside the store via the following relation

$$\mathrm{SHF} = \frac{h(T_\infty, W_c) - h(T_c, W_c)}{h(T_\infty, W_\infty) - h(T_c, W_c)} \tag{30}$$

where W is the humidity ratio of air. From the above equations it is clear that once $\dot{M}$ is determined, both Q_s and Q_L can be calculated because the conditions inside and outside the store are known.

NUMERICAL ANALYSIS AND COMPUTER CODE

Finite difference technique is used to discretize the governing equations and their boundary conditions. The power law is employed to discretize the convection-diffusion terms (Patankar 1980). The SIMPLER algorithm is adopted to solve the finite difference equations with stag-

gered grids to cover the integration domain (Patankar 1980). The integration domain is taken as the cross-sectional area of the cold store, in addition to an area of width B_1 outside the store (see Figure 2). This integration domain is bounded by nine surfaces as shown in the figure, and the conditions for θ, U, and V on these boundaries are depicted in Table 1. The thickness ΔD of the wall separating surfaces 3 and 9 is selected infinitesimally small ($\approx 10^{-4}$). The boundary conditions at surfaces 7 and 8 in Table 1 and Figure 2 need special attention since they differ from those given by Equation (20). In practice, the integration domain is finite and thus the conditions of U, V, and θ at $X \to \infty$ and $Y \to \infty$ can not be satisfied. In these cases the boundary conditions are replaced by those in Table 1, where it is assumed that the variations of U, V and are negligible in direction perpendicular to the surface.

Table 1. Boundary Conditions at Different Surfaces of Integration Domain (see Figure 2)

Surface	θ	U	V
1	$\theta = -1$	$U = 0$	$V = 0$
2	$\theta = -1$	$U = 0$	$V = 0$
3	$\theta = -1$	$U = 0$	$V = 0$
4	$\theta = -1$	$U = 0$	$V = 0$
5	$\theta = -1$	$U = 0$	$V = 0$
6	$\frac{\partial \theta}{\partial X} = 0$	$U = 0$	$V = 0$
7	$\begin{cases} V \le 0: \theta = 0 \\ V > 0: \frac{\partial \theta}{\partial Y} = 0 \end{cases}$	$\frac{\partial U}{\partial Y} = 0$	$\frac{\partial V}{\partial Y} = 0$
8	$\frac{\partial \theta}{\partial X} = 0$	$U = U^*$	$\frac{\partial V}{\partial X} = 0$
9	$\frac{\partial \theta}{\partial Y} = 0$	$U = 0$	$V = 0$

U^* is the value of U to satisfy the conservation of mass for the control volume with a face at the surface 9.

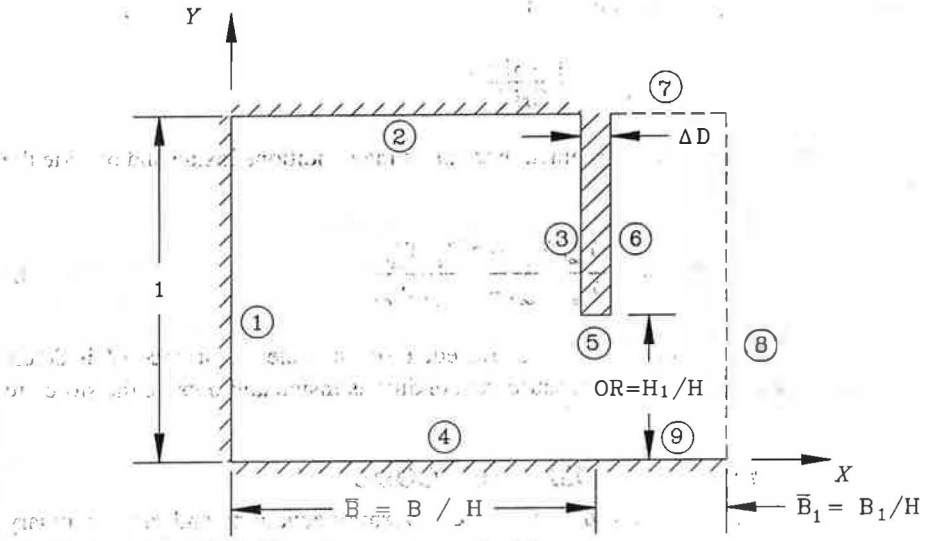

Figure 2. Domain of finite difference grid

A computer code "COLD.FOR" was prepared and validated against the results published in the literature for several engineering applications. Among the problems that were used to validate the computer code is the buoyancy driven flow in a square closed cavity with the vertical opposing walls are isothermal at two different temperatures, while the upper and lower walls are adiabatic (Krane and Jessee 1983, Barakos et al. 1994). Another case of validation is the buoyancy driven flow in a vertical open cavity with the vertical wall opposing to the opening is isothermal while the upper and lower walls are adiabatic (Chan and Tien 1985). In all cases fair agreement was obtained by the present computer code in comparison with other work in the literature. This suggests that the present model is valid for the type of flows compared.

The width $\bar{B}_1$ is introduced into the grid to account for the air motion of the infiltrated air outside the cold store. This motion definitely affects the flow pattern at the doorway and consequently affects the calculation of the rate of infiltrated air through the doorway. As $\bar{B}_1$ is increased, more accurate calculations are obtained, but on the expense of computation time. The testing of the results recommended to take $\bar{B}_1 = 0.4$ as a compromise between accuracy of results and computation time.

Also, three grids were used to test the dependence of the solution on the grid refinement. The values of ΔX and ΔY for these grids are given in Table 2. The testing of the results recommended the use of Grid B which is a compromise between accuracy of the results and computational time (Elsayed 1996). The convergence of the solution was found to also depend on the time steps $\Delta\tau$. The accuracy of a converged solution was improved by reducing the time step, but this of course on the expense of increasing the computation time. When operating at high Grashof number, the time step $\Delta\tau$ to give a dependable converged solution was found to be too small to the level that it excessively increases the computation time. An example is a case with $Gr = 10^{10}$, $OR = 0.5$, $\bar{B}_1 = 0.4$ and with a grid having $\Delta X = 0.1$ and $\Delta Y = 0.005$. Several computer runs were carried out using different values of $\Delta\tau$. It was found that at $\Delta\tau = 0.5 \times 10^{-6}$, the solution became practically independent of $\Delta\tau$. Computations were carried out on a supermini computer (scalar mode). The CPU time required for the previous example to reach time level of $\Delta\tau = 5$ starting from $\Delta\tau = 0$ was 5665 hours, which is equivalent to about 9 months of CPU time.

Table 2. Spacing of Various Grids with $\bar{B}_1 = 0.4$ as Used in Testing Computation Accuracy

Grid	ΔX	ΔY
A	0.2	0.1
B	0.1	0.05
C	0.1	0.033
D	0.05	0.033

PRACTICAL VALUES OF Gr AND THE TIME SCALE

In the introduction, three correlations from the literature were introduced. In the present work the prediction of the infiltration rate is determined in terms of Gr and *OR*, whereas the correlations given by Equations (3) to (5) use the values of T_∞, T_c, and H_1 as parameters, which are related to Gr as follows

$$Gr = \frac{\rho^2 \beta \Delta T}{\mu^2}\left(\frac{H_1}{OR}\right)^3 \tag{31}$$

where $\Delta T = (T_\infty - T_c)$. Also, the dimensionless time τ is related to the physical time t through the following relation

$$t = \frac{H}{\sqrt{g\beta\Delta T H}}\tau = \frac{\rho H^2}{\mu\sqrt{\mathrm{Gr}}}\tau \tag{32}$$

In practice, the temperature difference can become as high as 100°C in special types of very low temperature cold rooms. The height H of normal cold rooms varied between 2 and 4 m. However, small heights of 10 or 20 mm can represent a gap in a closed door that is not well sealed. The opening ratio OR can be as high as 1.0 for cases where the doorway extends to the ceiling, and it may become a very low fraction in some cases where H_1 is considered as the doorway 'undercut' or gap.

RESULTS

In the present section a parametric study is carried out to test the effect of changing
a. Grashof number Gr
b. Periods for which the door is kept open τ
c. Ratio of doorway height to room height, i.e. opening ratio OR.

In carrying out the parametric study grid B in Table 2 is used with $\Delta\tau = 0.5 \times 10^{-6}$. In cases "a" and "b" above, a room with $OR = 0.5$ is used.

Flow Pattern

The flow pattern was studied in terms of the dimensionless stream function Ψ, which is related to the dimensional stream function as follows

$$\psi = \mu\rho u_{ref} H\Psi \tag{33}$$

Calculations are carried out for rooms with and $OR = 0.5$ and $\mathrm{Gr} = 10^5$, 10^7, and 10^{10}. Figure 3 shows the variation of the flow pattern (lines of constant) for the case with $\mathrm{Gr} = 10^{10}$ at $\tau = 0.25$, 0.5, 1.0, and 5.0 from the instant to open the door. In this case, it was found that when steady state conditions are achieved, i.e. fully developed flow is established. Generally it was found that regardless of the value of Gr, the infiltration flow is initiated at the doorway due to the difference in the density of the air outside and inside the room (Elsayed 1997). Due to this difference in density, a recirculating flow is established with the center of the recirculation at the doorway. As the time τ increases, the recirculation of the flow becomes stronger and its effect extends deeper in the cold room till it reaches the cold wall facing the doorway (see Figure 3). The confinement of the recirculation of the infiltrated air by this cold vertical wall causes the birth of a secondary recirculating flow at right upward corner of the room (the zone behind the doorway wall, i.e. behind wall 3 in Figure 2). The behavior of the flow pattern was found to be independent of the value of Gr. The effect of increasing Gr manifests itself in increasing the strength of the recirculating flow which causes to bring more outside air into the cold room (Elsayed 1997).

Velocity Distribution at the Doorway

The distributions of the U component of the velocity at the doorway are shown in Figure 4 at $\mathrm{Gr} = 10^{10}$, for a cold room with $\overline{OR} = 0.5$. Other plots for $\mathrm{Gr} = 10^5$ and 10^7 are given by Elsayed (1997). In the figure, the velocity distributions are given at four time levels; mainly at $\tau = 0.25$, 0.5, 1.0, and 5.0. From the figure one may conclude the following:

1. The local magnitude of U at the doorway increases as τ increases up to $\tau = 1.0$. Then this magnitude decreases as τ increases. This means that the rate of air infiltration to the cold room reaches its maximum value at the early stages of opening the door, then this rate decreases to reach its steady state (fully developed flow) value.

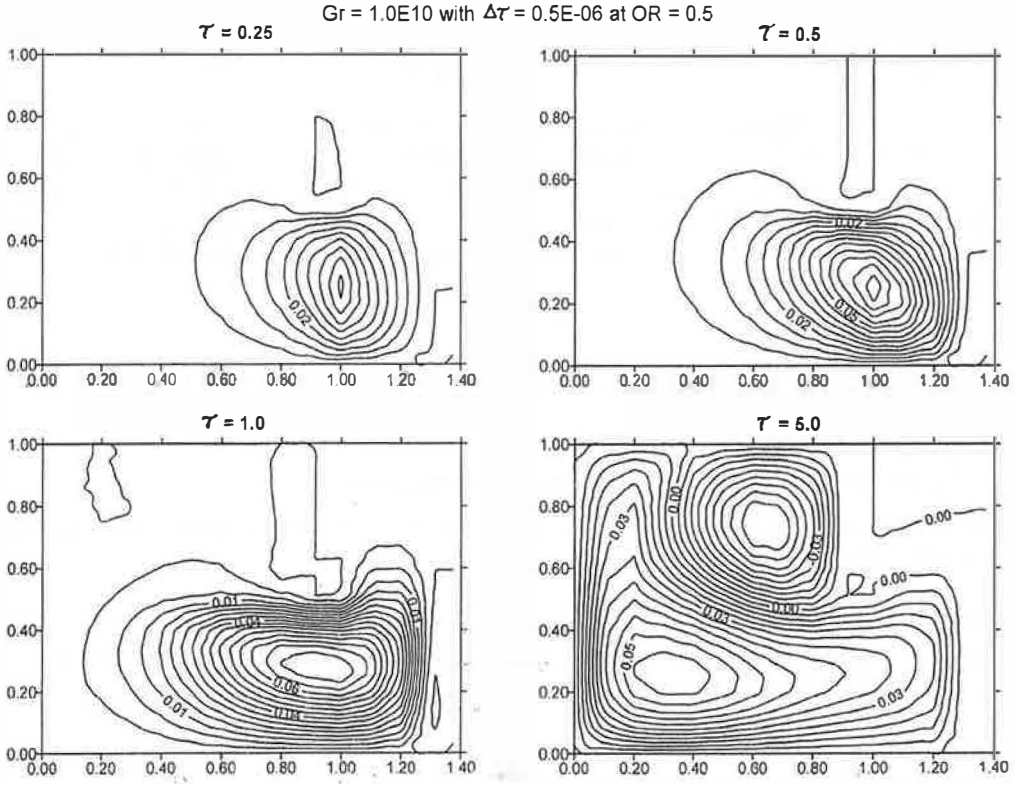

Figure 3. Flow pattern (lines of constant stream function) at Gr = 10^{10} for *OR* = 0.5

2. The point of zero value of U, i.e. point of reflection of the direction of U exists at a point slightly higher than the midpoint of the doorway. As Gr increases, the point of $U = 0$ becomes closer to the doorway midpoint, but as τ increases, approaching its steady state value, the point of $U = 0$ moves upwards, away from the doorway midpoint [Elsayed 1997].
3. As the flow proceeds to reach steady state conditions (i.e. fully developed flow), the velocity distribution at the doorway approaches a linear distribution. This behavior is encouraged by increasing Gr [Elsayed 1997].
4. As expected, warm air from outside enters the room in the upper part of the doorway and cold air leaves the room at the lower part of the room. Due to conclusion 2 above, the inflow to the room is slightly faster than the outflow, as also demonstrated by the figure.

Temperature Contours

The dimensionless temperature contours (curves of constant value of θ) are shown in Figure 5 for Gr = 10^{10}. Initially, the contours are vertical lines parallel to the doorway. At $\tau = 0$, the vertical doorway plane separates between the outside region at $\theta = 0$ and the cold room region at $\theta = -1$. As τ increases, the contours are deviated from being vertical. The outside region in front of the doorway gets colder as τ increases, while the upper outside region (region above the level of the doorway) stayed for some time unaffected, i.e. at $\theta \approx 0$. As the flow is developed to reach its final stage of fully developed flow (steady state conditions), the upper outside region is also cooled (i.e. it becomes affected by the flow leaving the cold room). However, increasing Gr diminishes this effect, i.e. makes the upper outside region is less affected by out going cold air (Elsayed 1997).

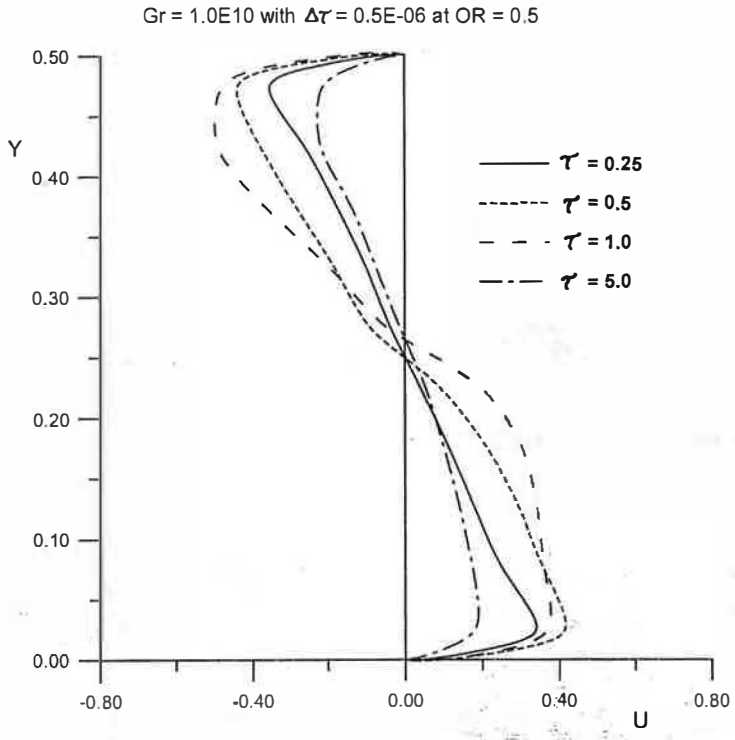

Figure 4. Velocity distribution at doorway with Gr = 10^{10} for *OR* = 0.5

Temperature Distribution at the Doorway

The development of the distribution of the dimensionless temperature θ with the dimensionless height Y at the doorway are given in Figure 6 for Gr = 10^{10}. As τ increases, the inflow to the room becomes colder because part of the cold outflow recirculates back to the room. This trend continues till fully developed flow is accomplished at steady state conditions, where the inflow temperatures reach their coldest values. Of course, the drop in the inflow air temperature leads to reducing the sensible load due to infiltration. This subject is further discussed in the next section.

Infiltration Load

The calculation of the cooling load due to infiltration is discussed in section 3. This load is determined in terms of its sensible part Q by the following relation

$$Q = Q_s/\text{SHF} \tag{34}$$

The value of Q_s is determined by Equation (26) after the modified mass rate $\dot{m}$ of infiltration air is determined from Equation (27). That is, Q is determined once $\dot{M}$ is determined.

Figure 7 depicts the variation of $\dot{M}$ with the increase in τ for Gr = 10^{10}. The general trend of this variation is that $\dot{M}$ increases with the increase in τ up to time τ^*, then decreases with the increase of τ. When steady state conditions are approached the rate of decrease in $\dot{M}$ diminishes until it reaches a constant value. The explanation for this behavior is given as follows in terms of the velocity and temperature distributions at the doorway (Figures 4 and 6) and with the help of the discussion given previously in this section.

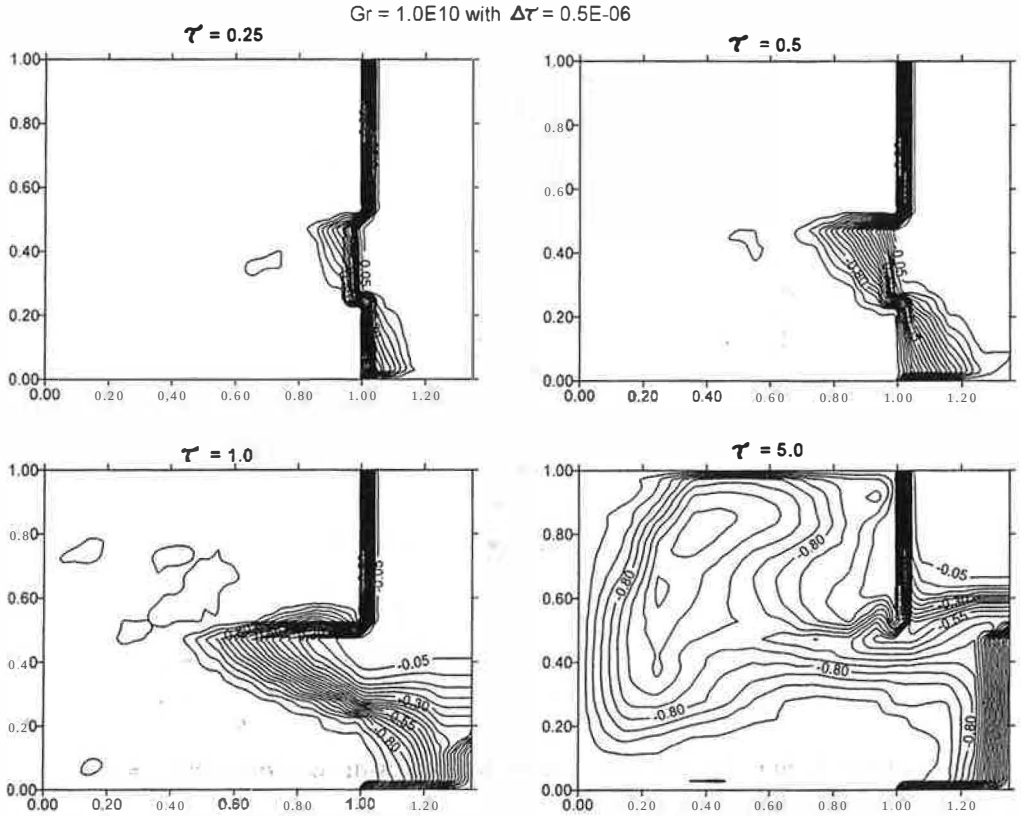

Figure 5. Isotherm at Gr = 10^{10} for *OR* = 0.5

Initially as τ increases, the magnitude of U at the doorway increases, and the difference in the temperature between the inflow and the outflow remains at its largest value (there is a slight decrease in this difference). The result of this trend is the increase of $\dot{M}$ with the increase in τ. When τ reaches τ^* the effect of flow confinement in the cold room; the rise in the temperature in the cold room zone near the doorway; and the recirculation of a part of the outflow back to the room cause the magnitude of U to decrease and the temperature difference between inflow and outflow to decrease. This leads to the decrease of $\dot{M}$ with the increase of τ until fully developed flow is accomplished. Figure 8 depicts the variation of τ^* with Gr. Figure 7 also includes a plot of the value $\dot{M}_{ss}$ calculated using the correlation prepared by Gosney and Olama (1975) [Equation (3)]. The value of $\dot{M}_{ss}$ from the correlation compares well with the maximum value of $\dot{M}$ predicted by the present work. The decrease in the infiltration rate in the present work after reaching its maximum value is because of the flow confinement caused by the vertical wall opposite the doorway; as discussed in the section describing flow patterns. It is believed that as the aspect ratio is reduced, the effect of this confinement is also reduced. For cold rooms with $AR << 1$, one would expect that the effect of the confinement becomes negligible, and this causes $\dot{M}$ to continuously increase with time until steady-state conditions are reached. Therefore, the difference between the present work and the correlation of Gosney and Olama (1975) is due to the effect of the flow confinement in the cold room that was not accounted for by Gosney and Olama.

The agreement between $(\dot{M})_{max}$ and $\dot{M}_{ss}$ from the correlation is explained as follows. The correlation of Gosney and Olama was developed assuming non-viscous, one dimensional fully

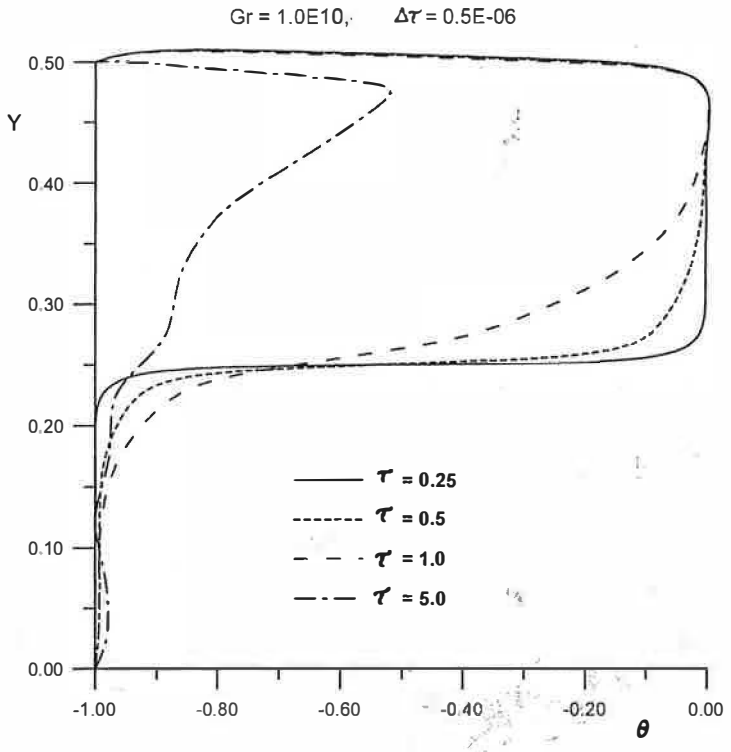

Figure 6. Temperature distribution at doorway with Gr = 10^{10} for OR = 0.5

developed flow, and constant temperatures for the inflow and outflow. These assumptions are found to be satisfied at early values of t where the effect of flow confinement in the room is not appreciable yet, i.e. at $\tau < \tau^*$ as demonstrated in the discussion in the previous sections. Once τ increases beyond τ^*, the above assumptions become incorrect and $\dot{M}$ decreases with the increase of τ for the reasons given previously, and thus $\dot{M}$ deviates from the value of $\dot{M}_{ss}$ predicted by the correlation.

Effect of Opening Ratio

Computer runs were carried out for a room with Gr = 10^{10} and OR = 0.25. The results are shown in Figures 9 to 13. The flow pattern (lines of constant) are plotted in Figure 9 for and τ = 0.25, 0.5, 1.0, and 5.0. By comparison with the flow pattern at OR = 0.5 shown in Figure 3, one finds that although the flow pattern at early times are the same, these patterns become completely different from one another when steady state conditions are achieved (τ = 5). At OR = 0.5 there is two cells in the cold store as shown in Figure 3. When OR is reduced to 0.25, the two cells are combined together into one cell with its center at the mid vertical plane as shown in Figure 9. As also shown, much less outside flow is infiltrated to the cold room through the doorway, at steady state conditions, as OR is reduced (compare Figures 3 and 9 at τ = 5.0). This is better explained by comparing the velocity distribution at the doorway at OR = 0.5 given by Figure 4 to that at OR = 0.25 given by Figure 10. It is clear from the comparison that at steady-state conditions (τ = 5.0) the infiltrated air flow rate is reduced as OR is reduced for two reasons. First, because the area of the doorway is reduced, and second because the magnitude of the maximum velocity of the infiltrated air is also reduced.

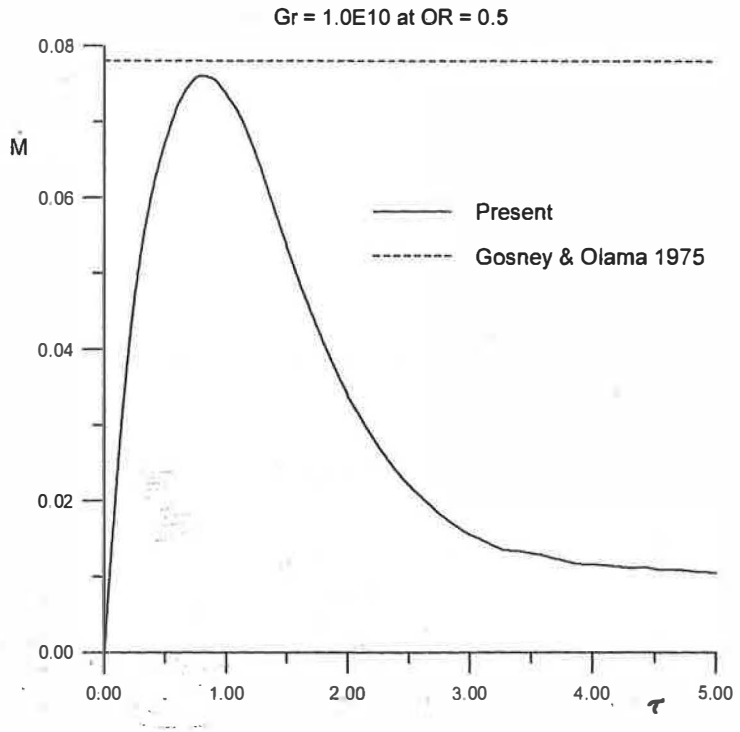

Figure 7. Variation of infiltration rate with time at Gr = 10^{10} for *OR* = 0.5

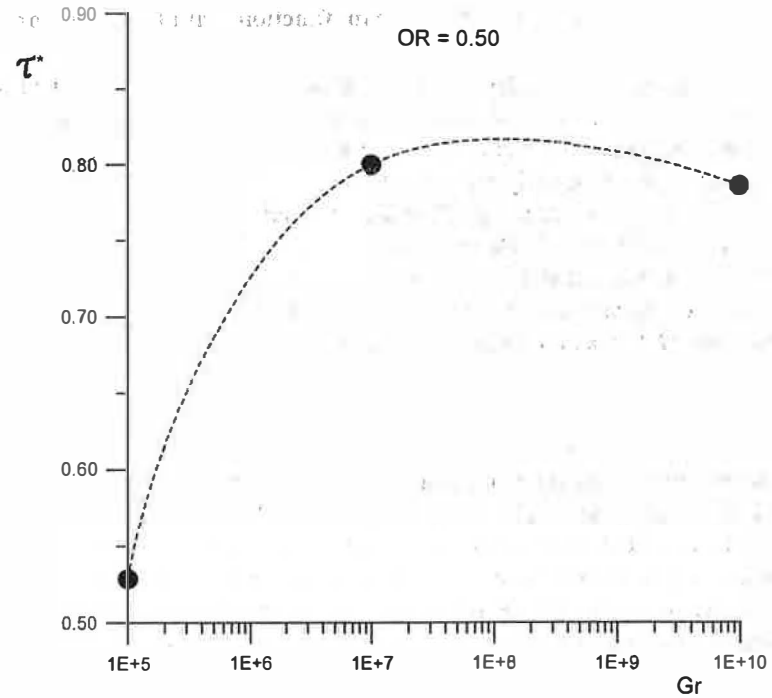

Figure 8. Variation of τ* with Gr for *OR* = 0.5

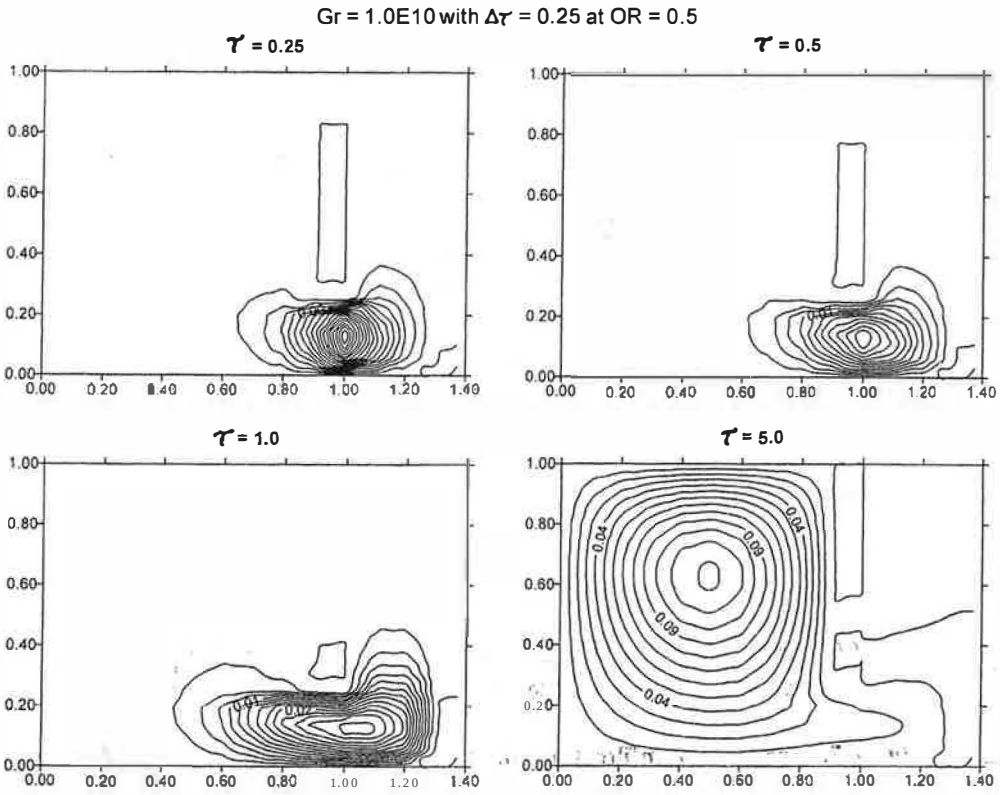

Figure 9. Flow pattern (lines of constant stream function) with Gr = 10^{10} for $OR = 0.25$

The comparison of the dimensionless temperature contours in Figures 5 and 11 at $OR = 0.5$ and 0.25, respectively, reveals that reducing OR brings the variation in the temperature caused by the infiltration to near the front part of the cold room, i.e. near the doorway. The temperature distribution at the doorway is slightly affected by the reduction in the value of OR as shown by Figures 6 and 12. The effect of reducing OR on the time variation of the infiltration rate through the doorway is shown in Figure 13. The peak value of $\dot{M}$ at $OR = 0.25$ is found to be about one third that of $\dot{M}$ at $OR = 0.5$. The trend of deviation of $\dot{M}$ from the steady-state value provided by the correlation of Gosney and Olama (1975) is almost the same for both $OR = 0.5$ and $OR = 0.25$. The time τ^* for $\dot{M}$ to reach its peak value is not dependent on the value of OR as shown in the figure.

Flow Factor

Many engineers currently calculate the infiltration rates through the doorway of a cold room using Equation (2) as recommended by ASHRAE (1994). In this equation, ASHRAE recommends that the doorway flow factor D_f range between 0.8 and 1.1, depending on the temperature difference between the cold store and the infiltrated air. This is a very crude determination of D_f. In the following discussion, the present results are used to predict the value of the doorway flow factor in a more detailed way. Referring to Equation (2), D_f is defined as follows

$$D_f = \int_0^t \dot{m}dt/\dot{m}_{ss} = \int_0^\tau \dot{M}d\tau/\dot{M}_{ss} \tag{35}$$

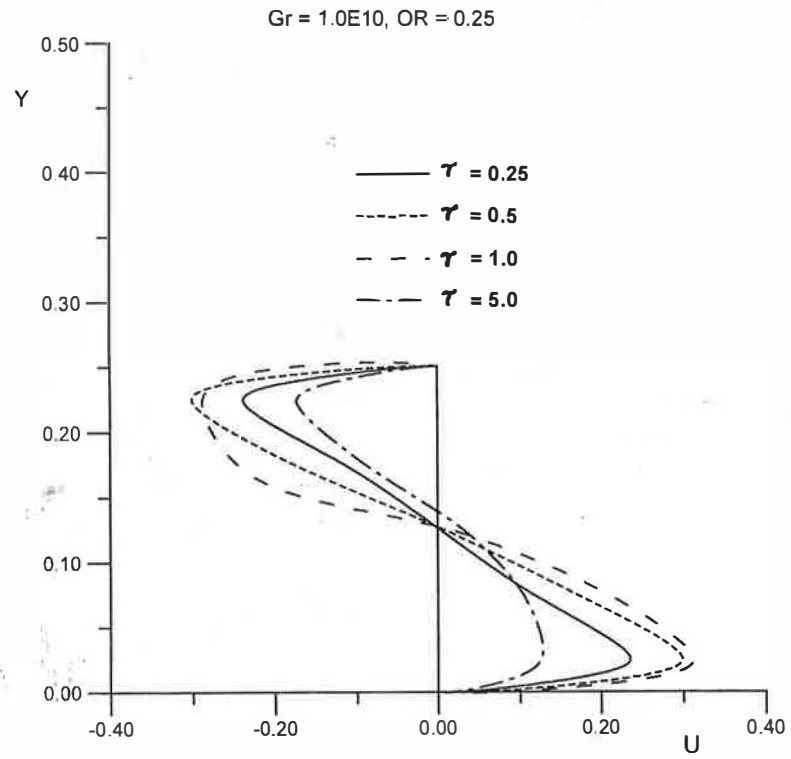

Figure 10. Velocity distribution at doorway with Gr = 10^{10} for *OR* = 0.25

where $\dot{m}_{ss}$ is the steady-state infiltration rate to the room through the doorway, $\dot{m}$ is the instantaneous value of the infiltration rate, and t is the duration for which the door is kept open. The integration in the numerator of Equation (35) was calculated numerically using a trapezoidal rule. The results of the computation were plotted in Figure 14, with the value of $\dot{m}_{ss}$ calculated from the present work. As shown, D_f depends on Gr, *OR*, and τ, and this dependence diminishes as τ increases.

At $\tau \geq 1.5$, the value of D_f decreases with the increase of τ, as given by Figure 15. As shown by the figure, a single correlation (broken line) was suggested to predict D_f at different values of τ. This correlation was given as follows

$$D_f = 6\tau^{-0.526} \tag{36}$$

The difference in the calculated value of D_f and the predicted one from the above correlation diminish as steady state conditions are approached. Figure 15 also includes the recommended range of D_f by ASHRAE (1994). Again the calculated and the correlation predicted values of D_f get closer to this range as steady state conditions are approached. We should note here that the recommend range of D_f by ASHRAE is based on experimental measurements which did not account for the effect of changing Gr or *OR*. At practical ranges of τ (high values of τ), the recommended range by ASHRAE underpredicts the value of D_f.

The steady state infiltration rate $\dot{M}_{ss}$ is plotted against the Grashof number Gr in Figure 16. As shown by the figure, a power relation is found between $\dot{M}_{ss}$ and Gr for a cold room with *OR* = 0.5. The correlation is given in the following form

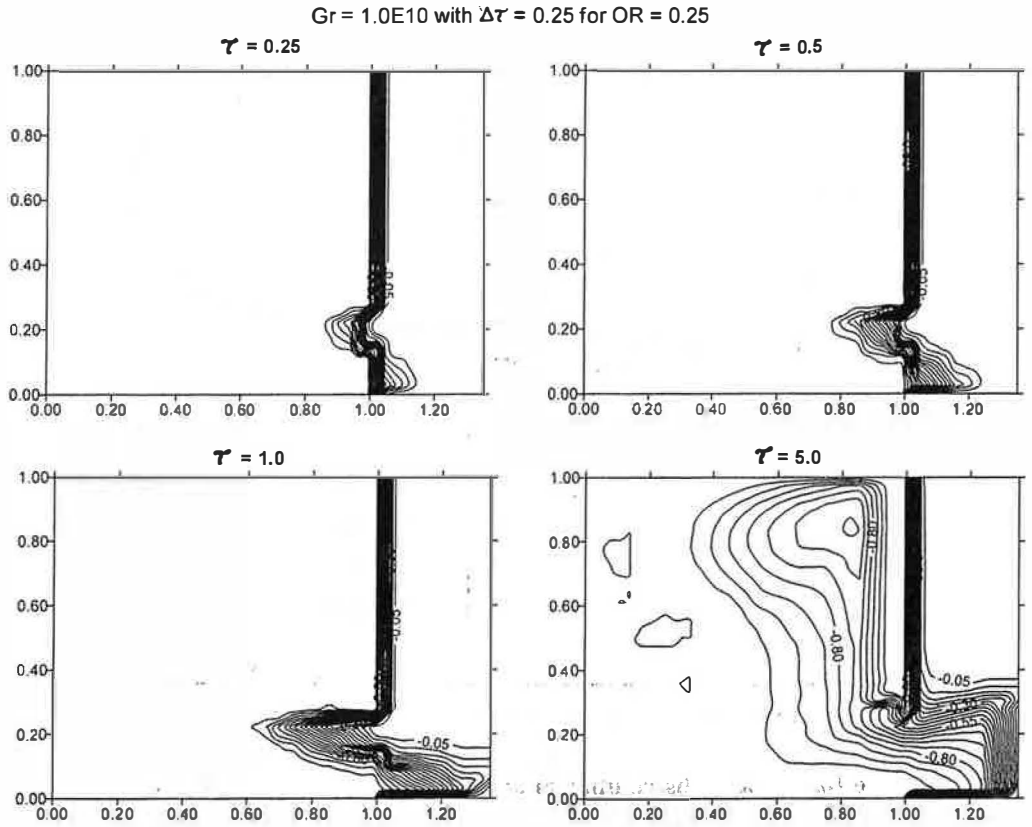

Figure 11. Isotherms at Gr = 10^{10} for *OR* = 0.25

$$\dot{M}_{ss} = 0.012 \tag{37}$$

The figure also shows a plot for the variation of $\dot{M}_{ss}$ with Gr when $\dot{M}_{ss}$ is calculated using the correlation of Gosney and Olama (1975), and the correlation of Jones et al. (1983). As shown in the figure, the correlation of Gosney and Olama (1975) and that of Jones et al. (1983) overpredict the value of $\dot{M}_{ss}$. As an example, using a room with $AR = 1$, $OR = 0.5$ and $Gr = 10^{10}$, the value of $\dot{M}_{ss}$ predicted by Equations (3) and (4) are about 7.3 and 8.3 times the predicted value of the present work, respectively.

COMPARISON WITH HEAT TRANSFER IN OPEN CAVITIES

Buoyancy driven flow in open cavities are of special interest in several engineering applications among which are solar receivers, air conditioning of buildings, electronic equipment, etc. Another engineering application is cold rooms which are the subject of the present work. This problem of buoyancy driven flow was studied by several researchers using cavities at various values of Rayleigh number, various boundary conditions at the walls of the cavity, and different geometries which include several combinations of the values of *AR* and *OR* for cavities with centered openings or off-center openings. Table 3 depicts some of the work available in literature for heat transfer in open cavities. As shown by the table, all the previous work were done for open cavities warmer than the surrounding except the present work which is for a cavity

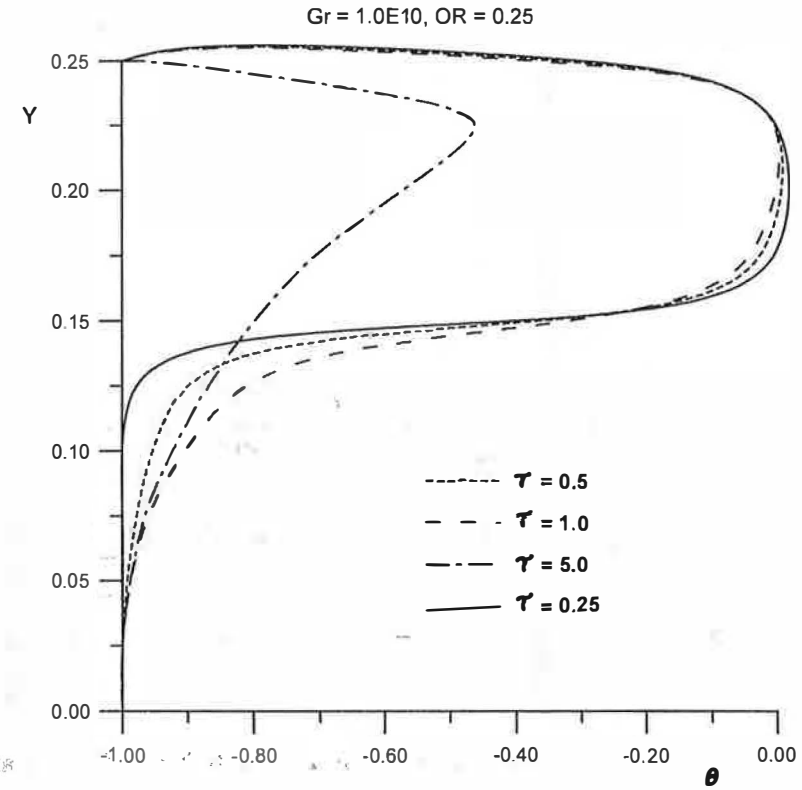

Figure 12. Temperature distribution at doorway with Gr = 10^{10} for *OR* = 0.25

colder than the surrounding. Generally, an average Nusselt number of the cavity can be defined as follows

$$\overline{\mathrm{Nu}} = \bar{h}H/k \tag{38}$$

where $\bar{h}$ is the average heat transfer coefficient between the cavity and the surrounding. In the present work, the value of $\bar{h}$ is determined from the following relation

$$\bar{h}HL(T_\infty - T_c) = \dot{m}_{ss}C_p(T_\infty - T_c) \tag{39}$$

Using Equation (27), the above equation yields

$$\overline{\mathrm{Nu}} = \mathrm{Gr}^{1/2}\mathrm{Pr}\dot{M}_{ss} \tag{40}$$

where the subscript *ss* indicates steady-state conditions.

Figure 17 compares the variation of $\overline{\mathrm{Nu}}$ with the Rayleigh from the present work and the literature. As shown by the figure, the present results compare well with those in the literature. On the same figure, the variations of $\overline{\mathrm{Nu}}$ with Ra as reduced from the correlation of Gosney and Olama (1975) are also shown. It is clear that this correlation over predicts the value of $\overline{\mathrm{Nu}}$ and thus over predicts the rate of infiltration to cold rooms in comparison with other work in the literature. It is therefore recommended to use Equation (37) instead of Equation (3) in the estimation of infiltration load to cold rooms.

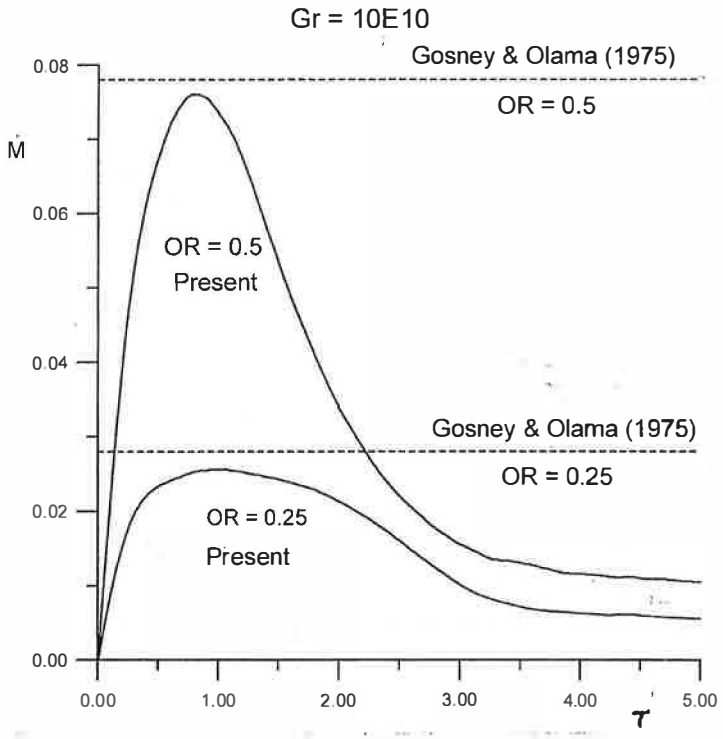

Figure 13. Variation of infiltration rate with time at Gr = 10^{10} for *OR* = 0.25 and 0.5

Table 3. Review of Previous Work on Fully/Partially Open Cavities

Reference		Geometry		B.C.[a]	Pr	Gr or Ra
		AR = *H*/*B*	*OR* = H_1/H			
LeQuere et al.	1981	1	1	A	0.73	$10^4 \le Gr_H \le 10^7$
		0.5, 2	1	A	0.73	$Gr_H = 10^7$
Penot	1982	1	1	A	0.7	$10^3 \le Gr_H \le 10^7$
Miyamoto et al.	1989	1	0.5, 1	A	0.7	$7 \times 10^3 \le Ra_B \le 7 \times 10^4$
		1	0.5, 1	A	0.7	$1 \le Ra_B \le 7 \times 10^5$
Showole and Tarasuk	1993	0.25, 0.5, 1	1	A	0.7	$10^4 < Ra_H < 5 \times 10^5$
		1	1	A	0.7	$10^3 < Ra_H < 5 \times 10^5$
Sernas and Kyriakides	1982	1	1	B	0.7	$Gr_H = 10^7$
Hess and Henze	1984	1	0.5, 1	C	7	$3 \times 10^{10} \le Ra_H \le 2 \times 10^{11}$
Chan and Tien	1985	0.143	1	C	1,7	$10^3 \le Ra_H \le 10^7$
Chan and Tien	1986	0.143	1	C	8.7	$10^6 \le Ra_H \le 10^8$
Angirasa et al.	1992	1	1	C	0.1-100	$10^2 \le Ra_H \le 10^8$
Lin and Xin	1992	1	1	C	0.7	$Ra_H = 10^{10}, 10^{11}$
Mohamad	1995	0.5, 1, 2	1	C	0.7	$10^3 \le Ra_H \times 10^7$
Chakroun et al.	1997	0.25, 0.5, 1	0.25, 0.5, 1	C	0.7	$Gr_H = 5.5 \le 10^8$
Present[b]		1	0.25, 0.5	C	0.7	$10^5 \le Ra_H \le 10^{10}$

[a]Boundary Conditions: A = all walls at T_w, B = all walls at T_w except upper wall is at T_∞,
C = all walls are adiabatic except wall facing the opening is at T_w or having constant heat flux.
[b]The opening of the cavity is not at the center, it is in the lower part of the cavity.

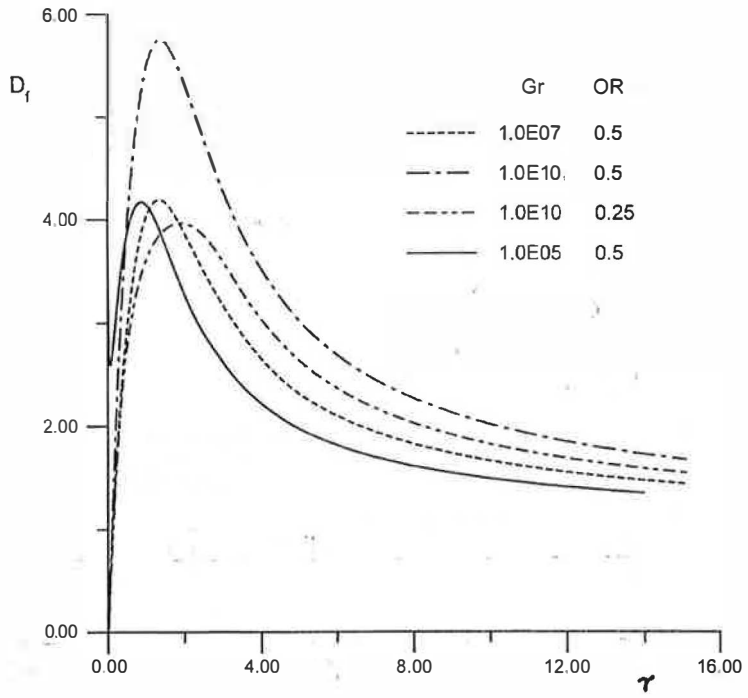

Figure 14. Variation of flow factor with time
(Based on steady-state flow obtained from present work)

CONCLUSIONS

A computer code using a two dimensional model is prepared to predict the infiltration load through doorways. The program is validated against known solutions in the literature for buoyancy driven cavity flows (closed and open cavities). The code is then used to predict the flow pattern and temperature distribution in cold rooms at any time from the instance of door opening. Also, the code is employed to predict the time variation of the infiltration rate to the room and the doorway flow factor. The study was carried out for a square cold room with $OR = 0.5$ for $Gr = 10^5$, 10^7, and 10^{10}; and with $OR = 0.25$ for $Gr = 10^{10}$. Our studies reveal the following conclusions.

1. The flow pattern and the temperature distribution caused by infiltration through the doorway are dependent on the Grashof number Gr and the opening ratio OR.
2. The variation of the infiltration flow rate $\dot{M}$ with the time τ measured from the instance of opening the door showed that for cold rooms with $AR = 1$, $10^5 \leq Gr \leq 10^{10}$, and $0.25 \leq OR \leq 0.5$, $\dot{M}$ increases with the increase of τ up to time τ^* after which $\dot{M}$ decreases as τ increases, until steady state conditions are achieved.
3. The correlation of Gosney and Olama (1975) overpredicts the infiltration rate $\dot{M}_{ss}$ at steady state conditions compared to the predicted values by the present model. This makes the results of the correlation of Gosney and Olama are questionable since this correlation is derived using a small-scale experimental model utilizing CO_2 and air to represent the differing densities as would be encountered as a result of temperature difference. Also, the effect of flow confinement was not considered in developing the correlation of Gosney and Olama. We believe that the difference between the present work and the predicted values by the correlation of Gosney and Olama will decrease for rooms with $AR < 1$.

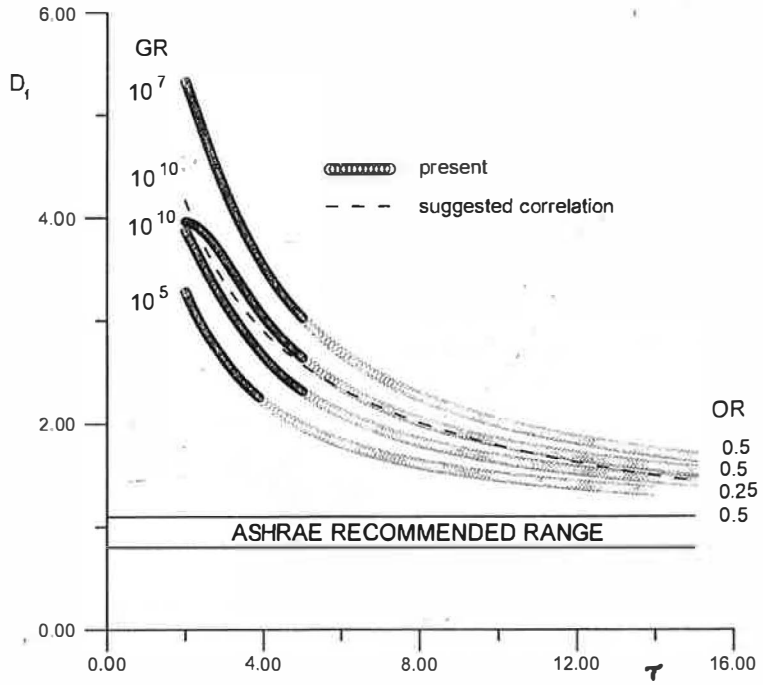

Figure 15. Variation of doorway flow factor with time
(Based on steady-state flow obtained from present work)

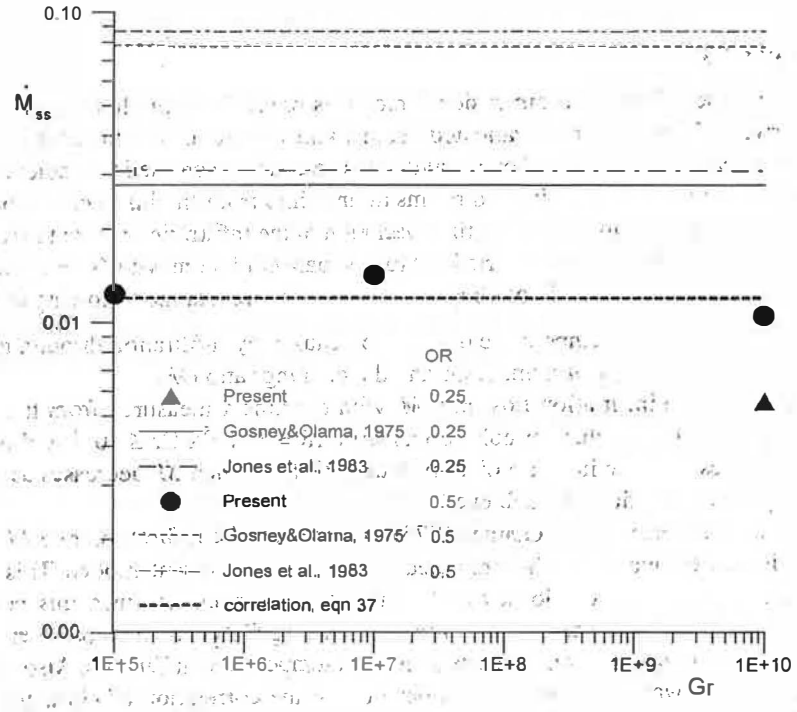

Figure 16. Comparison between variation of infiltration rate with Grashof number using present work and literature

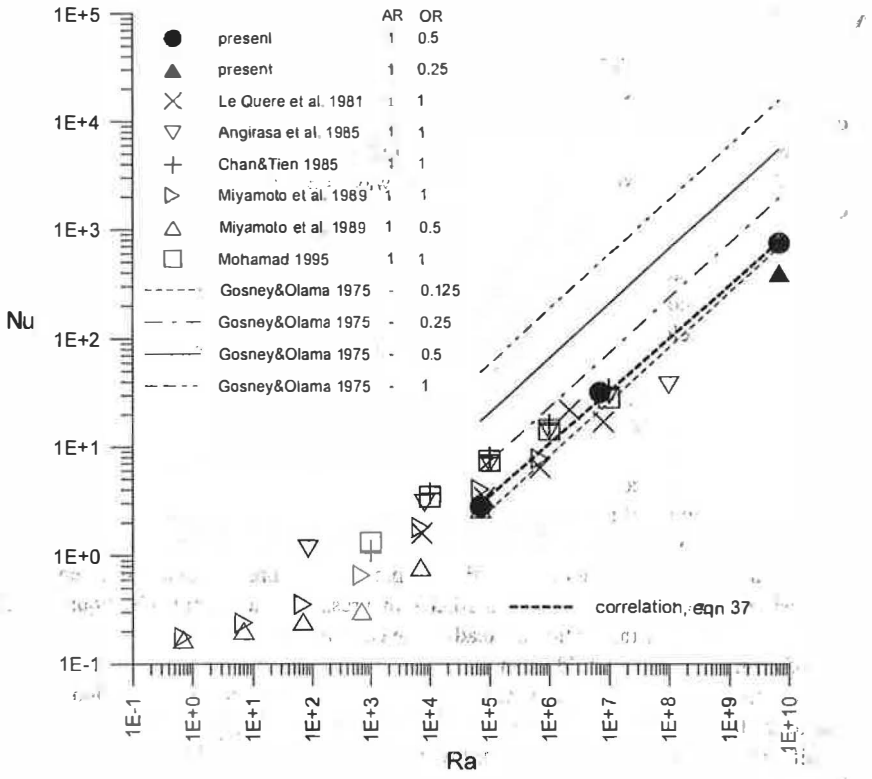

Figure 17. Variation of Nu with Ra in open cavities

4. The value of the opening ratio *OR* is found to affect the infiltration rate $\dot{M}$.
5. Though ASHRAE (1994) recommended that the flow factor D_f falls between 0.8 and 1.1 depending on the temperature difference between the cold room and the infiltrated air, the present work showed that D_f depends on both Gr and *OR*. At high values of τ (practical range of τ), the present calculation gave higher values of D_f than those recommended by ASHRAE. However our predicted values of D_f approach the recommended range of ASHRAE as τ increases.
6. Two correlations are derived from the present work: one to predict the doorway flow factor [Equation (36)], and the other to predict the infiltration rate through the doorway at steady state conditions [Equation (37)].
7. The heat transfer results of the present work compare well with the data in the literature for open cavities (Figure 17).

The present work pointed out the importance of carrying out more research to improve the accuracy of the prediction of the cooling load due to infiltration from the doorway of a cold room. The results presented here are one step in this direction.

ACKNOWLEDGMENT

This work is carried out for Project EM 097 sponsored by the Research Administration of Kuwait University.

NOMENCLATURE

AR	aspect ratio of the room, = H/B
B	width of cold room, see Figure 1
$\bar{B}$	dimensionless width, = B/H
B_1	width extension outside the doorway, see Figure 2
$\bar{B}_1$	dimensionless width extension outside the doorway, = B_1/H
C_p	specific heat of air at constant pressure
D_t	door open-time factor
D_f	doorway flow factor
E	effectiveness of doorway protective device
g	gravitational acceleration
Gr	Grashof number = $\rho^2 g\beta(T_\infty - T_c)H^3/\mu^2$
H	height of cold room, see Figure 1
H_1	height of doorway, see Figure 1
h	enthalpy
$\bar{h}$	average heat transfer coefficient
k	thermal conductivity of air
L	length of doorway
$\dot{M}$	dimensionless modified rate of infiltration air predicted by present model as given by Equation (27)
$\dot{M}_a$	dimensionless rate of infiltration air predicted by present model as given by Equation (23)
$\dot{M}_{ss}$	dimensionless rate of infiltration at steady state conditions
$\dot{m}_{inf}$	rate of infiltration air to a cold room
$\dot{m}_{ss}$	rate of infiltration air to a cold room at steady state conditions for fully open door
$\dot{m}_a$	rate of infiltration air to a cold room
$\dot{m}$	modified rate of infiltration air to a cold room
Nu	Nusselt number, = $\bar{h}\,H/k$
OR	opening ratio, = H_1/H
P	dimensionless pressure, see Equation (10)
p	pressure
Pr	Prandtl number, = $\mu\,C_p/k$
Ra	Rayleigh number, = Pr·Gr
Q	total infiltration load
Q_s	sensible part of infiltration load
Q_L	latent part of infiltration load
SHF	sensible heat factor, see Equation (28)
T	temperature
t	time
U	dimensionless velocity component in x direction, see Equation (10)
u	velocity component in x direction
V	dimensionless velocity component in y direction see Equation(10)
v	velocity component in y direction
W	humidity ratio of air
X	dimensionless distance along x direction, see Equation (10)
x	distance along the x direction, see Figure 1
Y	dimensionless distance along y direction, see Equation (10)
y	distance along the y direction, see Figure 1
β	coefficient of thermal expansion
θ	dimensionless temperature, see Equation (10)
μ	dynamic viscosity of air
ρ	density of air
τ	dimensionless time, see Equation (10)
ψ, Ψ	dimensionless stream functions

Subscripts

c cold room condition
∞ conditions outside cold room
ref reference value

Superscripts

+ indicates that only positive values of integrand is considered in the integration
* indicates instance when infiltration rate reaches its maximum value

REFERENCES

Angirasa, D. M., J.B.M. Pourquie, and F.T.M. Nieuwstadt. 1992. Numerical Study of Transient and Steady Laminar Buoyancy-Driven Flows Heat Transfer in a Square Open Cavity, *Numerical Heat Transfer,* 22A: 223-239.

ASHRAE. 1994. *ASHRAE Handbook—Refrigeration.* Atlanta: ASHRAE

Barakos, G., E. Mitsoulis, and D. Assimacopoulos. 1994. Natural Convection Flow in a Square Cavity Revisted: laminar and turbulent models with wall functions, *Int. J. for Numerical Methods in Fluids* 18: 695-719.

Chakroun, W., M.M. Elsayed, and S.F. Al-Fahed. 1997. Experimental Measurement of Heat Transfer Coefficient in a Partially/ Fully Open Tilted Cavity. *Trans. ASME, JSEE* Vol. 119 (4): 298-303.

Chan, Y.L., and C.L. Tien. 1985. A Numerical Study of Two-Dimensional Laminar Natural Convection in Shallow Open Cavities. *Int. J. Heat Mass Transfer* 28: 603-612.

Chan, Y.L., and C.L. Tien. 1986. Laminar Natural Convection in Shallow Open Cavities. *J. Heat Transfer* 108: 305-309.

Cole, R.A. 1984. Infiltration: A Load Calculation Guide. In *Proc. of International Institute of Ammonia Refrigeration,* Sixth Annual Meeting.

Elsayed, M.M. 1996. Development of Two Dimensional Model to Predict Infiltration Load in Cold Rooms. In *Proc. of the First U.A.E. Conference on Air Conditioning in the Gulf.* U.A.E. University, Al-Ain, U.A.E., pp 85-105.

Elsayed, M.M. 1997. Infiltration Load in Cold Rooms, Final Report of Project No. EM 097, Kuwait: Research Administration of Kuwait University.

Gosney, W.B., and H.A. Olama. 1975. Heat and Enthalpy Gains through Cold Rooms Doorways. In *Proc. of Institute of Refrigeration, Environmental Science and Technology.* The Polytechnic of the South Bank, London.

Hess, C.F., and R.H. Henze. 1984. Experimental Investigation of Natural Convection Losses from Open Cavities. *J. Heat Transfer* 106: 333-338.

Jones, B.W., B.T. Beck, and J.P. Steele.1983. Latent Loads in Low-Humidity Rooms due to Moisture. *ASHRAE Transactions* 89(1A): 35-55.

Krane, R.J., and Jessee. 1983. Some Detailed Field Measurements for Natural Convection Flow in a Vertical Square Enclosure. In *Proc. 1st ASME-JSHE Thermal Engineering Joint Conf.* 1: 323-329.

LeQuere, P., J.A.C. Humphrey, and F.S. Sherman. 1981. Numerical Calculation of Thermally Driven Two-Dimensional Unsteady Laminar Flow in Cavities of Rectangular Cross Section. *Numerical Heat Transfer* 4: 249-283.

Lin, C.X., and M.D. Xin. 1992. Transient Turbulent Free Convection in an Open Cavity. Institution of Chemical Engineers Symposium Series 1: 515-521.

Miyamoto, M., T.H. Keuhn, R.J. Goldstein, and Y. Katoh. 1989. Two-Dimensional Laminar Natural Convection Heat Transfer from a Fully or Partially Open Square Cavity. *Numerical Heat Transfer* 15A: 411-430.

Mohamad, A.A. 1995. Natural Convection in Open Cavities and Slots. *Numerical Heat Transfer* 27A: 705-716.

Patankar, S.V. 1980. *Numerical Heat and Fluid Flow.* Hemisphere: New York.

Penot, F. 1982. Numerical Calculation of Two-Dimensional Natural Convection in Isothermal Open Cavities. *Numerical Heat Transfer* 5: 421-437.